

Continuous parameter working memory in a balanced chaotic neural network

Nimrod Shaham¹ and Yoram Burak^{1,2}

¹*Racah Institute of Physics, The Hebrew University of Jerusalem*

²*Edmond and Lily Safra Center for Brain Sciences, The Hebrew University of Jerusalem*

(Dated: November 13, 2018)

Working memory, the ability to maintain and use information for several seconds, is central to many functions of the brain. In the context continuous variables, an important theoretical model of working memory is based on neural networks, whose dynamics possess a continuum of marginally stable steady states. It has been unclear whether this theoretical idea is compatible with one of the main proposals for the architecture of cortical circuits, the balanced network. Here we study a network with random connectivity which generates a balanced state. We find an architecture for which the network has a continuum of balanced states, in the limit of many neurons and many synapses per neuron. Finite networks can sustain slow dynamics in a certain direction in the mean activities space, but the chaotic dynamics drive diffusive motion along the line attractor, which gradually degrades the stored memory. We analyse the coefficient of diffusion along the attractor, and show that it scales inversely with the system size. For a large enough (but realistic) network size, and with suitable tuning of the network connections, it is possible to obtain persistence over time intervals which are larger by several orders of magnitude than the single neuron time scale.

Our brain is able to perform tasks that demand precision, while using highly fluctuating and noisy hardware. The irregular dynamics observed in single neuron activity is often modeled as arising from noisy inputs, or from intrinsic noise in the dynamics of single neurons. Another proposal for the source of noise in cortical circuits, is that it arises primarily from chaotic dynamics at the network level. In balanced networks [1, 2], chaotic activity induces apparent stochasticity in the activity of single units, despite the absence of intrinsic random noise.

Here we study the effect of chaotic noise on continuous parameter working memory, a task which is particularly sensitive to noise. Attractor dynamics are one of the main proposals for the neural activity underlying this task. The dynamics of continuous attractor networks are characterized by a continuum of marginally stable steady states, which allow for memorizing of parameters with a continuous range of values [3–7]. In such networks, noise can cause diffusion along the manifold of steady states, leading to degradation of the stored memory [8–11]. Most previous studies of stochastic effects on continuous attractor dynamics assumed intrinsic random noise in the neuronal activity or in the input, or in both. This raises the question, whether similar effects of noise will be observed if noise arises from chaotic dynamics in a balanced state.

The broad question, whether balanced networks can produce persistent activity has attracted considerable theoretical interest in recent years. Several works used a mechanism of clustered connections to obtain slow dynamics [12–14]. Others used short term synaptic plasticity [15, 16], or used different synaptic time scales to generate slow dynamics through a derivative feedback mechanism [17, 18]. Yet, previous works did not demonstrate analytically the existence of a continuum of balanced states in a neural network, and it remains unclear

whether such a continuum can be obtained without evoking additional mechanisms, such as short-term synaptic plasticity or derivative feedback. Here we demonstrate analytically that slow dynamics are attainable in a simple form of a balanced network, and address quantitatively how the chaotic nature of neural activity affects the ability of the neural network to store information about a continuous parameter.

Our neural network model is based on the classical balanced network model which was studied in Refs. [1, 2]. This model consists of two distinct populations, one inhibitory and the other excitatory. The recurrent connectivity is random with a probability K/N for a connection, where N is the population size (assumed for simplicity to be the same in both populations), K is the average number of connections per neuron from each population, and the connection strength is $\sim 1/\sqrt{K}$. The neuron activity (0 or 1) is determined in each update by the sign of the total input to the neuron minus a threshold. For $1 \ll K \ll N$ and over a wide range of parameters, the mean population activity settles to a fixed point (the *balanced state*) where on average the total excitation received by each neuron is approximately canceled by the total inhibition. The single neuron activity appears noisy, neither of the populations is fully activated or deactivated, and the overall network state is chaotic.

Despite the nonlinearities involved in the dynamics of each neuron, the population averaged activities in the balanced state are linear functions of the external input [1, 2]. We make use of this linearity to build a simple system of two balanced networks projecting to each other. The intuition comes from a simple model of a continuous attractor neural network, consisting of linear neurons arranged in two populations that mutually inhibit each other, Fig. 1(a). The linear rate dynamics of this system

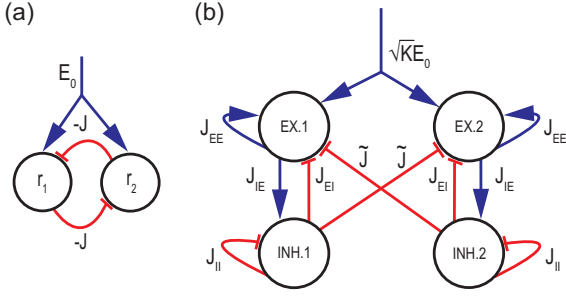


FIG. 1. (a) Two neural populations with rates r_1 , r_2 inhibit each other with synaptic efficacies $-J$. (b) Two coupled balanced subnetworks, each consisting of an excitatory and inhibitory population of N neurons. Connections within each network are random with connection probability K/N , $1 \ll K \ll N$. Connection strengths are: J_{EE}/\sqrt{K} , J_{IE}/\sqrt{K} , J_{EI}/\sqrt{K} and J_{II}/\sqrt{K} according to the identity of the participating neurons. Without loss of generality, we choose $J_{EE} = J_{IE} = 1$ and define $J_{EI} \equiv -J_E$, $J_{II} \equiv -J_I$. Mutual inhibition is generated by all-to-all connections of strength $-\tilde{J}\sqrt{K}/N$ from each inhibitory population to the excitatory population of the other subnetwork. An excitatory input $\sqrt{K}E_0$ is fed into both excitatory populations.

are given by:

$$\tau \dot{\vec{r}} = -\vec{r} + W\vec{r} + \vec{E}, \quad (1)$$

where $\vec{E} = [E_0, E_0]$, $E_0 > 0$ is an external input and

$$W = \begin{pmatrix} 0 & -J \\ -J & 0 \end{pmatrix}. \quad (2)$$

For $J = 1$ the system has a vanishing eigenvalue, and the fixed points form a continuous line: $r_1 + r_2 = E_0$.

In our model, a balanced subnetwork replaces each of these populations, and the inhibitory population in each network projects to the excitatory population of the other network, Fig. 1(b). As in [1, 2], the neurons are binary and are updated asynchronously, at update times that follow Poisson statistics. The mean time interval between updates is τ_E (τ_I) for neurons in the excitatory (inhibitory) population. In each update of a neuron k from population i , the new state of the neuron σ_i^k is determined based on the total weighted input to the neuron,

$$\sigma_i^k = \Theta(u_i^k), \quad (3)$$

where Θ is the Heaviside step function, and u_i^k is the total input to the unit at that time,

$$u_i^k = \sum_{l=1}^4 \left[\sum_{j=1}^{N_l} J_{kl}^{ij} \sigma_j^l(t) + \sqrt{K} E_0^l \right] - T_k. \quad (4)$$

Here, T_k is the threshold and E_0 is an external input. We chose the external input to be zero for the inhibitory populations and to be positive (and constant) for the excitatory populations. We denote by u_i the mean of u_i^k

over all the neurons k within the population i , and over the quenched noise. Similarly, we denote the variance of u_i^k by α_i . The mean field dynamics of the population averaged activities for $N \rightarrow \infty$ and $K \gg 1$ are given by:

$$\tau_i \dot{m}_i = -m_i + H(-u_i/\sqrt{\alpha_i}), \quad (5)$$

where $m_i(t) = 1/N \sum_{k=1}^N \sigma_i^k(t)$ [$i = 1$ (2) for the excitatory (inhibitory) population of the first subnetwork, and similarly $i = 3, 4$ in the second subnetwork] and $H(x)$ is the complimentary error function. We chose the mutual inhibition between the subnetworks to be all to all, and scale the interaction strength accordingly, so that the total input for each neuron scales with \sqrt{K} .

To check whether there exist parameters for which the system has a continuum of balanced states, it is convenient to write the steady state equations of the above dynamics as follows,

$$\begin{aligned} m_1 - J_E m_2 - \tilde{J} m_4 + E &= \frac{1}{\sqrt{K}} (T_1 - \sqrt{\alpha_1} H^{-1}(m_1)), \\ m_1 - J_I m_2 &= \frac{1}{\sqrt{K}} (T_2 - \sqrt{\alpha_2} H^{-1}(m_2)), \\ m_3 - J_E m_4 - \tilde{J} m_2 + E &= \frac{1}{\sqrt{K}} (T_1 - \sqrt{\alpha_3} H^{-1}(m_3)), \\ m_3 - J_I m_4 &= \frac{1}{\sqrt{K}} (T_2 - \sqrt{\alpha_4} H^{-1}(m_4)). \end{aligned} \quad (6)$$

Taking the limit $K \rightarrow \infty$, while demanding that none of the populations is fully on or off, produces a linear system of equations for the mean activities. By choosing the interaction strength between the two subnetworks to be $\tilde{J} = J_E - J_I$, this system becomes singular, and has a continuum of solutions, which represent a continuum of balanced states. Note that in order to have mutual inhibition, \tilde{J} should be positive, or $J_E > J_I$.

In the limit of infinite N and finite (but large) K , equations (6) are nonlinear, and a continuum of steady states cannot be established. Yet, if the nonlinear nullclines are close to each other, slow dynamics are attainable in a specific direction of the mean activity space. We note first that there always exists a symmetric fixed point, where $m_1 = m_3$ and $m_2 = m_4$. If in addition, at the symmetric point, the slopes of the nullclines are identical ($\partial m_3 / \partial m_1 = -1$), then there is a vanishing eigenvalue for the mean field dynamics, Eq. (5), at this point [19]. Under these conditions, the eigenvalue is expected to be small also in the vicinity of the symmetric point. In fact, even for moderately large values of K , the two nullclines nearly overlap over a large range of m_1 and m_3 , Fig. 2(b) ($K = 1000$). By requiring the existence of a vanishing eigenvalue in the linearized dynamics around the fixed point, it is possible to obtain a nonlinear equation for \tilde{J} , which we solve numerically. In the limit $K \rightarrow \infty$, the solution $\tilde{J} \rightarrow J_E - J_I$.

The stability of the approximate line attractor can be probed by numerically evaluating the eigenvalues of the linearized dynamics, in similarity to the stability analysis in [2]. For a large range of parameters, all four eigenvalues are negative. Thus, the approximate line attractor

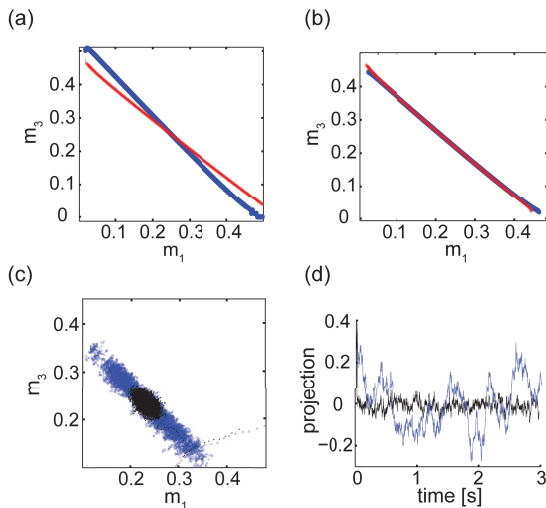


FIG. 2. (a) Nullclines in the $m_1 - m_3$ plane. $K = 1000$, $J_E = 4$, $J_I = 2.5$, $\tilde{J} = 1.5$, $\tau_E = 1$, $\tau_I = 0.8$, $E_0 = 0.3$. These values are used throughout the manuscript. (b) Same as (a), except that here \tilde{J} is tuned to ≈ 1.7 to achieve a singular Jacobian at the symmetric point. (c) Integration of equation (5) with injected uncorrelated Gaussian noise with standard deviation $\sigma = 10^{-2} 1/\sqrt{10\text{msec}}$, $\tilde{J} = 1.5$ (black), $\tilde{J} \approx 1.7$ (blue). (d) Dynamics of the projection along the special direction [parameters and colors as in (c)].

is stable. As an illustration for the existence of a direction in mean activity space along which the dynamics are slow, we artificially inject white noise to the system. Figs. 2(c), 2(d) show the dynamics for tuned and untuned mutual inhibition.

We next consider the realistic case where both N and K are finite (while still demanding $N \gg K \gg 1$). We performed numerical simulations of networks with N ranging between 10^4 to 12×10^4 . To simplify the analysis, we chose the random weights within each subnetwork such that they precisely mirror each other. This choice ensures that the fixed point is symmetric ($m_1 = m_3$ and $m_2 = m_4$) [20].

In our simulation, single neurons approximately exhibit exponential ISI distributions similar to those observed in the two population case. In contrast to the case of infinite N , in which we artificially injected noise into the system in order to drive motion along the attractor, for finite N we observe motion which is driven by the chaotic noise. Fig. 3(a) shows the averaged population activity, projected on the $m_1 - m_3$ plane. Fig 3(b) shows the projection along the slow direction: note that the motion along this line is slow, and is characterised by a timescale of ~ 1 s. To demonstrate that the dynamics are effectively one dimensional, a projection on a perpendicular direction is shown as well.

Let us define $X(t)$ to be the projection of the averaged population activities on the approximate attractor (where $X = 0$ at the symmetric fixed point). The dy-

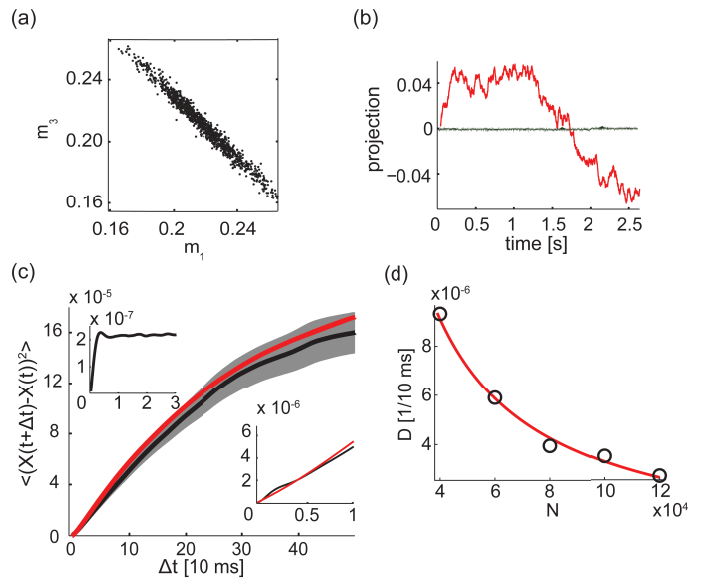


FIG. 3. (a) Projection of the mean activities on the $m_1 - m_3$ plane, for finite $N = 10^5$. (b) Dynamics of the projection along the special direction (red) and a perpendicular projection (black). (c) Measurements of $G(X, \Delta t)$ from simulations (black. Blue: std of the mean), compared with the semi-analytical approximation (Eq. (S28)) ($N = 1.2 \cdot 10^5$). Lower inset: zoom-in on $\Delta t \leq \tau$. Upper inset: similar measurements from a single, disconnected balanced network. (d) Diffusion coefficient as a function of N .

namics of X can be characterized as a stochastic process with the moments:

$$F(X, \Delta t) \equiv \frac{\langle X(t + \Delta t) - X(t) | X(t) = X \rangle_t}{\Delta t}, \quad (7)$$

$$G(X, \Delta t) \equiv \left\langle [X(t + \Delta t) - X(t)]^2 | X(t) = X \right\rangle_t. \quad (8)$$

Equation (7) characterizes the systematic drift along the attractor. For small Δt and near the fixed point, we expect $F(X, \Delta t) \approx -\lambda X$ with constant λ , characterising the timescale of decay towards the fixed point. In fact, we find that this relation holds to a very good approximation over a wide range of positions along the approximate attractor (Fig. S2). In simulations of the finite N network, we estimated λ from measurements of $F(X, \Delta t)$ near the symmetric point, and tuned \tilde{J} to obtain $\lambda^{-1} \gg \tau$, starting from the value of \tilde{J} for which $\lambda = 0$ in the mean field theory. In Fig. 3, $\lambda^{-1} \simeq 3$ s.

Equation (8) characterizes the random diffusion driven by the chaotic noise. Fig. 3C shows measurements of this quantity from simulations, for X near the symmetric fixed point. On short time scales compared to τ , G can be analytically approximated using the averaged autocorrelation function, $q_j(t) \equiv 1/N \sum_{i=1}^N \langle \sigma_i^j(t + \Delta t) \sigma_i^j(t) \rangle$. Using an expression for q , derived in Ref. [2] for a network

with a single fixed point, we obtain, for $\Delta t \lesssim \tau$,

$$G(X, \Delta t) \approx \frac{2\Delta t}{N} \sum_{j=1}^4 (v_j^0)^2 \left[-\frac{\partial q_j(t)}{\partial t} \right] \Big|_{t \rightarrow 0}, \quad (9)$$

where \bar{v}^0 is the left eigenvector of the system's Jacobian with eigenvalue close to zero (SM). We note that G is proportional to Δt and inversely proportional to N .

Similar scaling of $G(X, \Delta t)$ with N and Δt holds also in the single balanced network of Ref. [2], for $\Delta t \ll \tau$. However, in the case of a single balanced network, G saturates for $\Delta t \gtrsim \tau$ (upper inset in Fig. 3C). On time scales larger than τ , the behavior of our network differs dramatically from that of the single balanced network, since G continues to increase as a function of Δt , up to Δt of order λ^{-1} (Fig. 3C). Because the chaotic noise is uncorrelated on time scales larger than τ , and since λ is approximately constant along the attractor, we expect the motion to approximately follow the statistics of an Ornstein–Uhlenbeck (OU) process. Indeed, this approximation provides a good fit to the dynamics (Fig. S3). This allows to extract from the simulations a diffusion coefficient D , which characterises the random motion on time scales $\tau \lesssim \Delta t \lesssim \lambda^{-1}$.

In noisy continuous attractor networks, in which neurons are intrinsically and independently stochastic, the coefficient of diffusion along the attractor scales inversely with the system size [8]. This raises the question, whether similar scaling occurs when diffusion arises from the chaotic noise. Figure 3(d) demonstrates that the diffusion coefficient is indeed inversely proportional to N .

In general, analytical expressions for time dependent correlation functions that involve multiple neurons are not available in balanced networks (see [21] for further discussion). However, using the noise cross correlations measured in simulations of a single balanced network, we can obtain a semi analytical approximation for G . We first model the dynamics of a single balanced network as a two dimensional stochastic process, representing the activities of the excitatory and inhibitory populations. The network response to a temporally fluctuating input can be derived analytically from a linearization of the mean field dynamics around the symmetric fixed point. In addition, we include in the dynamics stationary random noise, which accounts for the chaotic fluctuations. The temporal correlation function of this noise is measured from simulations of a single balanced network. We next consider the dynamics of two such stochastic processes, when coupling the activity in each process to the external input of the other process. This procedure, described in detail in the SM, provides an excellent approximation for $G(0, \Delta t)$, Fig. 3(c). Thus, the statistics of diffusion along the attractor can be derived without fitting parameters, from the fluctuations observed in the single balanced network.

Finally, we briefly address the chaotic nature of the

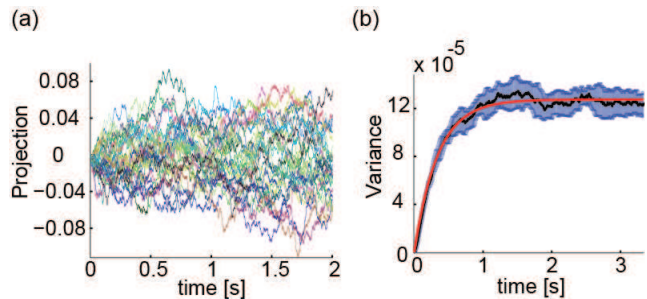


FIG. 4. (a) Projections of the mean activities over the special direction in 30 trials with the same update schedule and the same initial condition, except for one neuron which is flipped in each population ($N = 10^5$). (b) Variance over 1500 trials as a function of time, with 2σ errorbars. Red: fit to the variance of an OU process ($D \simeq 3.4 \cdot 10^{-6} \text{1/10s}$).

noise that drives diffusive motion. Figure 4(a) shows results from multiple simulations, in which the initial network state differed only by a flip of one neuron in each population (out of $\sim 10^5$ neurons). All other parameters, including the asynchronous update schedule and the network weights were identical across runs. The time dependence of the variance across different runs is similar to the variance over realizations of an OU process, Fig. 4(b), with similar diffusion coefficient as observed in the fit for $G(X, \Delta t)$ [Fig. 3(c)]. Thus, different initial conditions are equivalent to different realization of dynamic noise that drives diffusive motion along the line.

In summary, we find that slow dynamics along a continuous line in the population mean activity space are attainable in a balanced network. In finite networks, the chaotic dynamics of neural activity drive diffusive motion along the attractor, in similarity to the effect of noise that arises from intrinsic neural or synaptic mechanisms. Using analytical and numerical analysis, we show that the diffusion coefficient along the attractor is inversely proportional to the network size. Thus, the persistence of the network can be improved by increasing the number of neurons. In similarity to attractor networks with intrinsic neural noise [8], a fairly large number of neurons is required to suppress diffusion along the attractor and allow for stable representation of a memory. In practice, in a network with 10^5 neurons per population, diffusion over one second causes a deflection of $\sim 10^{-2}$ in units of mean activity, compared to a range of order unity. Thus, this network size is sufficient in our model, with proper tuning of the synaptic weights, to achieve persistence times of several seconds, much larger than the single neuron time scale.

This research was supported by the Israel Science Foundation grant No. 1733/13 and (in part) by grant No. 1978/13. We acknowledge support from the Gatsby Charitable Foundation, and from the Rudin Foundation (NS).

-
- [1] C. van Vreeswijk and H. Sompolinsky, “Chaos in neuronal networks with balanced excitatory and inhibitory activity,” *Science*, vol. 274, no. 5293, pp. 1724–1726, 1996.
- [2] C. van Vreeswijk and H. Sompolinsky, “Chaotic balanced state in a model of cortical circuits,” *Neural computation*, vol. 10, pp. 1321–1371, Aug. 1998. PMID: 9698348.
- [3] D. A. Robinson, “Integrating with neurons,” *Annual Review of Neuroscience*, vol. 12, no. 1, pp. 33–45, 1989. PMID: 2648952.
- [4] H. S. Seung, “How the brain keeps the eyes still,” *Proceedings of the National Academy of Sciences*, vol. 93, pp. 13339–13344, Nov. 1996. PMID: 8917592.
- [5] A. Compte, N. Brunel, P. S. Goldman-Rakic, and X.-J. Wang, “Synaptic mechanisms and network dynamics underlying spatial working memory in a cortical network model,” *Cerebral Cortex*, vol. 10, no. 9, pp. 910–923, 2000.
- [6] O. Barak, D. Sussillo, R. Romo, M. Tsodyks, and L. Abbott, “From fixed points to chaos: three models of delayed discrimination,” *Progress in neurobiology*, vol. 103, pp. 214–222, 2013.
- [7] O. Barak and M. Tsodyks, “Working models of working memory,” *Current Opinion in Neurobiology*, vol. 25, pp. 20–24, Apr. 2014.
- [8] Y. Burak and I. R. Fiete, “Fundamental limits on persistent activity in networks of noisy neurons,” *Proceedings of the National Academy of Sciences*, vol. 109, pp. 17645–17650, Oct. 2012. PMID: 23047704.
- [9] Z. P. Kilpatrick, B. Ermentrout, and B. Doiron, “Optimizing working memory with heterogeneity of recurrent cortical excitation,” *The Journal of Neuroscience*, vol. 33, no. 48, pp. 18999–19011, 2013.
- [10] K. Wimmer, D. Q. Nykamp, C. Constantinidis, and A. Compte, “Bump attractor dynamics in prefrontal cortex explains behavioral precision in spatial working memory,” *Nature neuroscience*, vol. 17, no. 3, pp. 431–439, 2014.
- [11] P. M. Bays, “Noise in neural populations accounts for errors in working memory,” *The Journal of Neuroscience*, vol. 34, no. 10, pp. 3632–3645, 2014.
- [12] A. Litwin-Kumar and B. Doiron, “Slow dynamics and high variability in balanced cortical networks with clustered connections,” *Nature neuroscience*, vol. 15, no. 11, pp. 1498–1505, 2012.
- [13] R. Rosenbaum and B. Doiron, “Balanced networks of spiking neurons with spatially dependent recurrent connections,” *Physical Review X*, vol. 4, no. 2, p. 021039, 2014.
- [14] M. Stern, H. Sompolinsky, and L. Abbott, “Dynamics of random neural networks with bistable units,” *Physical Review E*, vol. 90, no. 6, p. 062710, 2014.
- [15] G. Mongillo, O. Barak, and M. Tsodyks, “Synaptic theory of working memory,” *Science*, vol. 319, no. 5869, pp. 1543–1546, 2008.
- [16] D. Hansel and G. Mato, “Short-term plasticity explains irregular persistent activity in working memory tasks,” *The Journal of Neuroscience*, vol. 33, pp. 133–149, Jan. 2013. PMID: 23283328.
- [17] S. Lim and M. S. Goldman, “Balanced cortical microcircuitry for maintaining information in working memory,” *Nature Neuroscience*, vol. 16, pp. 1306–1314, Aug. 2013.
- [18] S. Lim and M. S. Goldman, “Balanced cortical microcircuitry for spatial working memory based on corrective feedback control,” *The Journal of Neuroscience*, vol. 34, no. 20, pp. 6790–6806, 2014.
- [19] See Supplemental Material at [URL will be inserted by publisher] for additional details.
- [20] When the connections in each subnetwork are chosen independently, the fixed point deviates slightly from this symmetry plane. All the qualitative results described below remain valid.
- [21] A. Renart, J. de la Rocha, P. Bartho, L. Hollender, N. Parga, A. Reyes, and K. D. Harris, “The asynchronous state in cortical circuits,” *science*, vol. 327, no. 5965, pp. 587–590, 2010.